Distinguishability in Impedance Imaging

Margaret Cheney and David Isaacson, *Member, IEEE*

Abstract—**Impedance imaging systems apply currents to the surface of a body, measure the induced voltages on the surface, and from this information, reconstruct an approximation to the electrical conductivity in the interior. This paper gives a detailed discussion of several ways to measure the ability of such a system to distinguish between two different conductivity distributions. The subtle differences between these related measures are discussed, and examples are provided to show that these different measures can give rise to different answers to various practical questions about system design.**

Introduction

THERE are many different ways of measuring the ability of an impedance imaging system to distinguish between different conductivity distributions. In fact, two infinite sets of numbers called "visibilities" and "sensitivities" were first introduced for this purpose in [19], [21]. In this paper, we discuss single-number measures such as that in [11], [12]. This paper describes several different single-number measures, shows how they can be used to study various questions, and compares the results obtained from the different measures.

Two conductivity distributions can be distinguished from one another when some applied current pattern induces boundary voltages that differ by more than the precision of the voltmeter. These boundary voltages can be made larger by applying more current. But any practical system will have a limitation on the amount of power that can be applied. This power limitation must be taken into account when one studies questions such as: 1) What is the best current pattern to distinguish one conductivity distribution from another? 2) What electrode size should be used? 3) What are the smallest inhomogeneities detectable with a given measurement precision? This paper discusses several ways of taking into account the power limitation, and shows that the answers to the above questions can depend on how this is done.

The first section of the paper contains a discussion of a mathematical idealization, the "continuum model," in which arbitrary current densities can be applied to the entire boundary. We show how limiting the applied power in this model leads naturally to the use of Sobolev norms and spaces. Sobolev spaces are a standard mathematical tool for measuring the size and smoothness of functions. In order to make this paper self-contained, we have included a tutorial on Sobolev norms and spaces in Appendix A, which may be read in conjunction with the first section.

This first section also contains a discussion of what happens when various norms are used in the definition of distinguishability. This results in different measures of a system's ability to differentiate between different conductivity distributions. The differences between these related concepts are discussed, and examples are provided to show that such subtle changes in the definition can give rise to different answers to various practical questions.

The second section of the paper describes a more practical model in which the current is applied through discrete electrodes. We develop several notions of distinguishability for this discrete case. We show that use of an inappropriate notion can lead to erroneous answers to certain questions.

The third section provides examples of different ways to compare the efficacy of different discrete current patterns in detecting a centered circular object at the center of a circular, homogeneous body.

Manuscript received June 3, 1991; revised February 10, 1992. This work was supported by the National Institutes of Health Research Grants GM39388, GM42935, and BRSG Grant RR-07104; by the National Science Foundation Grant EET 8706340; and by the Office of Naval Research Grant N-00014-89-J-1129.

The authors are with the Department of Mathematical Sciences, Rensselaer Polytechnic Institute, Troy, NY 12180.

IEEE Log Number 9201488.

I. The Continuum Case

A. Notation

To discuss the continuum case, we need the following notation. We consider a body B with surface S. The conductivity distribution in B we denote by σ. We will also need another conductivity distribution σ^0. The units of conductivity are, say, Mho/cm = 1/(ohm-cm). The electric potential u (units: volts) is assumed to satisfy the equations [13]

$$\nabla \cdot \sigma \nabla u = 0 \quad \text{inside the body } B \tag{1.1}$$

$$\sigma \frac{\partial u}{\partial \nu} = j \quad \text{on the surface } S. \tag{1.2}$$

Here j denotes the current density. The units of current density are, say, amps/cm^2. Conservation of charge implies that

$$\int_S j = 0. \tag{1.3}$$

The restriction of u to the boundary we denote by v. We choose a ground so that

$$\int_S v = 0. \tag{1.4}$$

We denote by R the "resistive" [11]–[13] map that takes j to v. For the case of the conductivity distribution σ^0, we denote the boundary values by v^0 and the corresponding resistive map by R^0.

In the following, we allow the conductivity to be complex, in order to include the case in which alternating currents are applied to the body [7], [13]. In this case, the conductivity σ should be replaced by $\sigma + i\omega\epsilon$ where ϵ is the electric permittivity and ω is the frequency.

B. Power

If we multiply the complex conjugate of (1.1) by u and use the divergence theorem, we obtain

$$\int_B \sigma|\nabla u|^2 = \int_S jv^* \tag{1.5}$$

where the star denotes complex conjugate. The real part of (1.5) is proportional to the power dissipated in the body. Requiring that this power be finite is essentially a requirement that u have finite H^1 norm in the interior where H^1 denotes the usual Sobolev norm. (See Appendix A for a short tutorial on Sobolev spaces.) The "trace" theorem [1] then tells us that v, the restriction to the boundary of u, is in $H^{1/2}$. Because v is one degree smoother than j [8], j must be in $H^{-1/2}$. From the definitions of the Sobolev spaces, we have that (1.5) and its real part, the power, satisfy the bound

$$\left|\int_S jv^*\right| \le \|j\|_{-1/2}\|v\|_{1/2} \tag{1.6}$$

where the norms are Sobolev norms defined in (A.5) of the Appendix. Appendix A also contains a short calculation that shows why (1.6) holds.

Using the $H^{-1/2}$ norm of j and the $H^{1/2}$ norm of v gives us precisely the boundary data with finite power, as can be seen in the following example.

Example 1.1: σ^0 = constant, B = cylinder of height 1 and radius 1.

We assume that $j = 0$ on the top and bottom of the cylinder, and that j is constant in the vertical direction. In this case (1.1) becomes Laplace's equation in two dimensions, which we can solve by separation of variables. If we denote by j_n the nth Fourier coefficient of j and by v_n^0 the nth Fourier coefficient of v^0, then we have $v_n^0 = j_n/(\sigma^0|n|)$. Parseval's identity [16] tells us that (1.5), the expression whose real part is proportional to the power, can be written in terms of the Fourier coefficients as

$$\int_S jv^* = 2\pi \sum{}' j_n(v_n^0)^* = 2\pi \sum{}' \frac{|j_n|^2}{\sigma^0|n|} \tag{1.7}$$

where the prime on the sum means that the $n = 0$ term is omitted [because of (1.3) and (1.4)]. This expression is equivalent to the square of the $H^{-1/2}$ norm of j (see Appendix). Similarly, we can express (1.5) in terms of v_n^0 rather than j_n as

$$\int_S j(v^0)^* = 2\pi \sum{}' \sigma^0|n|\,|v_n^0|^2. \tag{1.8}$$

This expression is equivalent to the square of the $H^{1/2}$ norm of v^0. Thus, the largest class of current densities j and voltage v with finite power are those in $H^{-1/2}$ and $H^{1/2}$, respectively.

C. Distinguishability

In [12], distinguishability is defined to be the norm of the voltage differences divided by the norm of the current density. But what norms should be used? A natural choice [11] is the $H^{1/2}$ norm for the voltage distribution and the $H^{-1/2}$ norm for the current density. Specifically, as in [11], we define $\delta_{1/2}$, the distinguishability in the $1/2$ sense, by

$$\delta_{1/2}(\sigma, \sigma^0, j) = \frac{\|v - v^0\|_{1/2}}{\|j\|_{-1/2}}. \tag{1.9}$$

From the definition (A.5) of the Sobolev norms, we see that $\delta_{1/2}$ has the units of resistivity, namely length times resistance. In addition, we note that $\delta_{1/2}$ is "homogeneous of degree zero," i.e., $\delta_{1/2}(j)$ remains the same when j is multiplied by a constant.

Definition (1.9) is a natural one because, as we saw above, the voltages must be in $H^{1/2}$ and the current density in $H^{-1/2}$. If we use these norms, we may be able to distinguish two conductivity distributions that we might not be able to distinguish if we used some other norms.

However, in studying certain questions, one can use other norms that are easier to work with. For example, in [9], the authors mainly used distinguishability in the mean square sense, namely δ_0, where

$$\delta_0(\sigma, \sigma^0, j) = \frac{\|v - v^0\|_0}{\|j\|_0} \tag{1.10}$$

where the norm is the L^2 norm

$$\|f\|_0^2 = \int_S |f|^2.$$

We see that δ_0 is also homogeneous of degree zero, but has different dimensions, namely resistance times area. Definition (1.10) can be related to (1.9) with the help of the inequality

$$\|f\|_{-1/2} \le \|f\|_0 \le \|f\|_{1/2}. \tag{1.11}$$

This inequality implies that definition (1.10) gives a smaller number than the one given by (1.9); i.e.,

$$\delta_0(\sigma, \sigma^0, j) \le \delta_{1/2}(\sigma, \sigma^0, j). \tag{1.12}$$

Another way to see that (1.10) gives a smaller distinguishability is to note that definition (1.10) does not allow all possible current densities. This is due to the fact that the space $H^{-1/2}$ is larger than L^2: L^2 functions are required to be smoother than $H^{-1/2}$ functions (see Appendix A).

However, the norm in (1.10) is easy to work with. In fact, (1.10) can be used to study certain questions, such as the question of which current densities are best for distinguishing a centered cylindrical object from its back-

ground. The following example shows that the answer to this question does not depend on whether (1.10) or (1.9) is used, although the numbers obtained for δ_0 and $\delta_{1/2}$ are different.

Example 1.2: A centered cylindrical object in a cylindrical body.

Suppose that B is a cylinder, and the current densities are such that the problem again reduces to a two-dimensional one. Let us consider the problem of distinguishing a centered circular object from a constant background σ^0. For both bodies, (1.1) can be solved by separation of variables [9]. This process shows that the eigenfunctions of both resistive maps R and R^0 are the same trigonometric functions $\exp in\theta$. We denote the corresponding eigenvalues by ρ_n and ρ_n^0, respectively. In other words, the Fourier coefficients of the voltage and current density are related by $v_n = \rho_n j_n$ and similarly for v_n^0. Then the nth Fourier coefficient of the difference in voltages is $\delta v_n = v_n - v_n^0 = (\delta\rho_n) j_n$, where $\delta\rho_n = \rho_n - \rho_n^0$. The $H^{1/2}$ norm of the voltage difference is therefore

$$\|\delta v\|_{1/2}^2 = 2\pi \sum{}' \sqrt{1 + |n|^2}\, |\delta\rho_n j_n|^2$$

$$= 2\pi \sum{}' (1 + |n|^2) |\delta\rho_n|^2 \frac{j_n^2}{\sqrt{1 + |n|^2}}. \quad (1.13)$$

In order to find a current density that best distinguishes σ from σ^0, we should maximize (1.13), subject to the condition that $\| j \|_{-1/2} = 1$. Since the difference $|\delta\rho_n|$ turns out to be largest when $n = \pm 1$, (1.13) can be maximized by choosing $j_1 = (2^{1/2}\pi)^{-1/2}$ and all other j_ns zero. In other words, j should be proportional to $\exp i\theta$. With this choice, the distinguishability is

$$\delta_{1/2}(\sigma, \sigma^0, e^{i\theta}) = \|\delta v\|_{1/2} = \sqrt{2}\, |\delta\rho_1|. \quad (1.14)$$

What happens if we do this same calculation using the L^2 norm? We have

$$\|\delta v\|_0^2 = 2\pi \sum{}' |\delta\rho_n j_n|^2 \le \max_n |\delta\rho_n|^2 \| j \|_0^2. \quad (1.15)$$

Again we see that (1.15) can be maximized, subject to the condition $\| j \|_0 = 1$, by taking $j_1 = 1$ and all other j_ns zero. Thus for a best current density we obtain a multiple of the one found above, namely $\exp i\theta$. The distinguishability, however, is

$$\delta_0(\sigma, \sigma^0, e^{i\theta}) = \sqrt{\max_n |\delta\rho_n|^2} = |\delta\rho_1| \quad (1.16)$$

which is smaller by a factor of $\sqrt{2}$ than the $\delta_{1/2}$ distinguishability computed above.

We could just as well have maximized (1.13) and (1.15) by taking any linear combination of $\exp i\theta$ and $\exp -i\theta$ whose norm is one. Thus, the current densities $\cos\theta$ and $\sin\theta$ (appropriately normalized) are the best current densities for distinguishing a centered disk for a homogeneous background [12] with both δ_0 and $\delta_{1/2}$ measures. (To actually make an image of the conductivity anomaly, however, more current densities would be required [4]. These other current densities could be chosen to correspond to the other eigenfunctions of R or $R - R^0$).

For other pairs of conductivity distributions, especially those differing on the boundary, the definition of distinguishability affects the best current densities. (This was mentioned but not discussed in detail in [11].) One can see this by noting that the maximum distinguishability is the largest $|\lambda|$ for which

$$(R - R^0) j = \lambda j \quad (1.17)$$

has a nonzero solution j, and such a j is a best current density [9].

A best current for $\delta_{1/2}$, however, is a j for which

$$\max_j \frac{\|(R - R^0) j\|_{1/2}}{\| j \|_{-1/2}} \quad (1.18)$$

is attained. The Sobolev norms in (1.18) can be written in terms of the natural Laplacian ("Laplace–Beltrami operator") on the surface S (see Appendix A for examples). In the case of the unit disk, the natural Laplacian is ∂_θ^2, and the expression (1.18) can be written

$$\max_j \frac{\|(1 - \partial_\theta^2)^{1/4}(R - R^0) j\|_0}{\|(1 - \partial_\theta^2)^{-1/4} j\|_0}. \quad (1.19)$$

This maximum is [5] the largest $|\lambda|$ for which

$$(1 - \partial_\theta^2)^{1/4}(R - R^0) j = \lambda (1 - \partial_\theta^2)^{-1/4} j \quad (1.20)$$

has a nonzero solution j. For general conductivity distributions, there is no reason that the js satisfying (1.17) should be the same as the js satisfying (1.20).

II. The Discrete Case

A. Notation

In practice, one cannot specify the current density (in $\mathrm{mA/cm^2}$, say), but rather one specifies only the currents (in mA) sent to the electrodes. These currents we denoted by I_l, $l = 1, 2, \cdots, L$. The induced voltages on the electrodes we denote by V_l, $l = 1, 2, \cdots, L$. We denote by $\mathcal{R}$ the "resistance" map that takes the "current pattern" $I = (I_1, I_2, \cdots, I_L)$ to the "voltage pattern" $V = (V_1, V_2, \cdots, V_L)$. We decorate these quantities with the superscript 0 when they are associated with the conductivity σ^0. We use the notation $\langle X, Y \rangle$ to denote the inner product $\Sigma X_l Y_l^*$, and the notation $\|X\|$ to denote the norm $\sqrt{\langle X, X \rangle}$.

B. Power

The power is proportional to the real part of

$$\sum_{l=1}^{L} I_l V_l^*. \quad (2.1)$$

C. Distinguishability

How should we define distinguishability in the discrete case? Again we should choose a definition that is homo-

geneous of degree zero. Although (1.11) suggests

$$\delta_I(\sigma, \sigma^0, j) = \sqrt{\frac{\sum_{l=1}^{L} |V_l - V_l^0|^2}{\sum_{l=1}^{L} |I_l|^2}}, \tag{2.2}$$

this definition does not directly take the power into account. A definition that explicitly normalizes by the power applied to σ^0 is

$$\delta_P(\sigma, \sigma^0, j) = \sqrt{\frac{\sum_{l=1}^{L} |V_l - V_l^0|^2}{\text{Re} \sum_{l=1}^{L} I_l (V_l^0)^*}}. \tag{2.3}$$

We note that (2.2) has the units of resistance, whereas (2.3) has the units of the square root of resistance. This suggests that the δ_I may behave differently from δ_P.

In certain special cases, definition (2.2) can be useful. One such case is in answering the question of which current pattern best distinguishes a centered cylinder object from its background [10].

Example 2.1: A centered cylindrical object in a cylindrical body.

We consider the same conductivity distribution as in Example 1.2, but this time, instead of looking for the best current densities, we look for the best current patterns. In this case a best current pattern for δ_I is one at which the maximum

$$\max_I \frac{\|(\mathcal{R} - \mathcal{R}^0)I\|}{\sqrt{\langle I, I\rangle}} \tag{2.4}$$

is attained, whereas a best current pattern for δ_P corresponds to

$$\max_I \frac{\|(\mathcal{R} - \mathcal{R}^0)I\|}{\sqrt{\text{Re}\ \langle I, \mathcal{R}^0 I\rangle}}. \tag{2.5}$$

In the δ_I case, the maximum is the largest magnitude eigenvalue of $\mathcal{R} - \mathcal{R}^0$, and a best current pattern is one of the corresponding eigenvectors. In the δ_P case, the maximum is the largest value of $|\lambda|$ for which

$$(\mathcal{R} - \mathcal{R}^0)I = \lambda\ \text{Re}\ \mathcal{R}^0 I \tag{2.6}$$

has a nonzero solution I, and one of the corresponding Is is a best current pattern. In the case when both conductivity distributions are rotationally invariant, the eigenvectors of both $\mathcal{R}$ and $\mathcal{R}^0$ are the same, namely the discrete trigonometric functions [3], [20]. The corresponding eigenvalues are computed in Appendix B for a particular mathematical model that accounts for the presence on the boundary of L conducting electrodes separated by nonconducting gaps. For this "gap" model, with conductivity in the interior corresponding to a centered circular object against a homogeneous background, it happens that the current patterns corresponding to the largest $|\lambda|$ satisfying (2.6) are the same as those corresponding to the largest magnitude eigenvalue of $\mathcal{R} - \mathcal{R}^0$. Thus, maxima of both (2.4) and (2.5) occur at multiples of the vector I^1 whose lth component is $I_l^1 = e^{i\theta_l}$ where $\theta_l = 2\pi l/L$ is the center of the lth electrode. In other words, current patterns giving the best distinguishability are in both cases multiples of the same I^1, irrespective of whether distinguishability is defined by (2.2) or (2.3). Again, $I^{-1} = e^{-i\theta_l}$ also maximizes (2.4) and (2.5), and so does any linear combination of I^1 and I^{-1}.

That (2.2) gives the same answer in this case is a happy accident. Even if the eigenvectors of $\mathcal{R} - \mathcal{R}^0$ are the same as the Is satisfying (2.6), there is no guarantee that the λs of (2.6) will be arranged in the same order as the eigenvalues of $\mathcal{R} - \mathcal{R}^0$. The following example shows how this can happen.

Example 2.2: Two different homogeneous distributions.

Here we again take the body to be the unit cylinder, but this time we take the two distributions to be the constants $\sigma = \sigma^1$ and σ^0, respectively. As before, we reduce the problem to a two-dimensional one. Since both distributions are invariant under discrete rotations, the corresponding resistance maps again have the discrete trigonometric functions as eigenfunctions. The eigenvalue of $\mathcal{R} - \mathcal{R}^0$ corresponding to the kth spatial frequency is $\rho_k^1 - \rho_k^0$ where ρ_k^0 is given by (B.7) and ρ_k^1 is the corresponding expression for σ^1. These eigenvalues are clearly decreasing as $|k|$ increases from 1 to $L/2$. Thus the current pattern that maximizes (2.4) is I^1, defined in the example above. These same eigenvalues and eigenvectors can be used in (2.6) to compute λ. Taking I equal to the kth eigenvector and solving for λ, we obtain

$$\lambda_k = \frac{\rho_k^1 - \rho_k^0}{\rho_k^0} = \sigma^0 \left(\frac{1}{\sigma^1} - \frac{1}{\sigma^0}\right).$$

This expression is independent of k, which means that all current patterns are equally good for distinguishing σ^1 from σ^0, when distinguishability is defined by (2.3).

For conductivity distributions that are not rotationally invariant, eigenvectors of $\mathcal{R} - \mathcal{R}^0$ are not necessarily the same as solutions of (2.6), and consequently the best current patterns for δ_P can differ from those for δ_I. Since δ_P reflects the limitations of a physical system, it is the better choice. For such general pairs of conductivity distributions, the best current patterns can be found by an experimental procedure such as that described in [10]. Because this procedure is based on the notion of distinguishability, the foregoing comments also apply to it. In particular, it is better to use (2.3) when studying changes on the boundary, because it is more sensitive to conductivity changes at the boundary.

For the study of questions involving changes on the boundary, δ_I is a very poor choice. An example of such a question is that of which electrode size gives the best distinguishability. The reason δ_I is such a poor choice is that for a fixed number of electrodes, the sum of the squares of the currents remains constant, no matter how big the electrodes are. If the electrodes are small enough, the current density and power both become arbitrarily large. The

calculation of the power in the small-electrode limit is done in Appendix B for the "gap model" formulation [3], [14].

III. Examples in the Discrete Case

In this section, we illustrate the use of discrete measures of distinguishability in the problem of predicting the size of the smallest centered object that can be distinguished from a homogeneous background (example 2.1). We can answer this question by considering the difference between the voltages for a homogeneous body of radius r_0 and for the same body containing an object of radius r_1:

$$V - V^0 = (\mathcal{R} - \mathcal{R}^0)I. \tag{3.1}$$

We will be able to detect the presence of the object if at least one $V_l - V_l^0$ is larger than the measurement precision of the voltmeter. We can compute the size of these voltage differences by expanding the I of (3.1) in the basis of normalized characteristic current patterns $T^k = I^k/\sqrt{L}$ where $I^k = e^{-ik\theta_l}$:

$$I = \sum_{k=-L/2}^{L/2-1}{}' \langle I, T^k \rangle T^k. \tag{3.2}$$

The voltage difference is then

$$V - V^0 = \sum_{k=-L/2}^{L/2-1}{}' \langle I, T^k \rangle (\mathcal{R} - \mathcal{R}^0)T^k. \tag{3.3}$$

Because the T^k are the eigenvectors of $\mathcal{R} - \mathcal{R}^0$ in this example, we need only compute the corresponding eigenvalues. These eigenvalues can be computed explicitly for a "gap model" formulation of the boundary conditions. For the case in which the electrodes each have area A and are equally spaced, each electrode subtending an angle w, computation of the eigenvalues ρ_k^0 of $\mathcal{R}^0$ is carried out in Appendix B; the eigenvalues ρ_k of $\mathcal{R}$, which are obtained in a similar way, are

$$\rho_k = \frac{Lr_0}{\pi A\sigma^0} \sum_{m=-\infty}^{\infty} \frac{(1 - \mu\Gamma^{2|k+mL|})}{(1 + \mu\Gamma^{2|k+mL|})} \frac{\operatorname{sgn}(k + mL)}{(k + mL)^2} \cdot \sin\frac{(k + mL)w}{2} \tag{3.4}$$

where $\Gamma = r_1/r_0$ and

$$\mu = \frac{\sigma^1 - \sigma^0}{\sigma^1 + \sigma^0}.$$

We denote the eigenvalues of the difference operator $\mathcal{R} - \mathcal{R}^0$ by $\delta\rho_k$. They are given by

$$\delta\rho_k = \frac{Lr_0}{\pi A\sigma^0} \sum_{m=-\infty}^{\infty} \frac{-2\mu\Gamma^{2|k+mL|}}{(1 + \mu\Gamma^{2|k+mL|})} \frac{\operatorname{sgn}(k + mL)}{(k + mL)^2} \cdot \sin\frac{(k + mL)w}{2}. \tag{3.5}$$

Knowledge of the eigenvalues enables us to compute (3.3) as

$$V - V^0 = \sum_{k=-L/2}^{L/2-1}{}' \langle I, T^k \rangle \delta\rho_k T^k. \tag{3.6}$$

In order to compute the voltage differences, we need only compute $\langle I, T^k \rangle$. We compute these quantities for the following current patterns.

Best Patterns

As we found in Example 2.1, the best current patterns in this case are I^1 and I^{-1}, or any linear combination of I^1 and I^{-1}. For I^1 and I^{-1},

$$\langle I^1, T^k \rangle = \begin{cases} \sqrt{L} & k = 1 \\ 0 & \text{otherwise} \end{cases}$$

and

$$\langle I^{-1}, T^k \rangle = \begin{cases} \sqrt{L} & k = -1 \\ 0 & \text{otherwise.} \end{cases}$$

Linear combinations of I^1 and I^{-1} that are natural to use are $B^{\pm} = (I^1 \pm I^{-1})/2$. These are $B_l^+ = \cos\theta_l$ and $B_l^- = \sin\theta_l$. For them we have

$$\langle B^{\pm}, T^k \rangle = \begin{cases} \sqrt{L}/2 & k = 1 \\ \pm\sqrt{L}/2 & k = -1 \\ 0 & \text{otherwise.} \end{cases} \tag{3.7}$$

A Walsh Pattern

A current pattern W that has the advantage of requiring only current generators that put out two different currents is

$$W_l = \begin{cases} 1 & l = 1, 2, \cdots, L/2 \\ -1 & l = L/2 + 1, \cdots, L. \end{cases}$$

This is an example of a discrete Walsh function [17]. Here we have assumed L to be even. In this case, we have

$$\langle W, T^k \rangle = \left(\sum_{l=1}^{L/2} e^{ik\theta_l} - \sum_{l=L/2+1}^{L} e^{ik\theta_l} \right) \Big/ \sqrt{L}. \tag{3.8}$$

We can compute the sums by writing them as geometric series with ratio $\exp 2\pi ki/L$. For $k = -L/2 + 1, \cdots, 0, \cdots, L/2 - 1$, (3.8) becomes

$$\langle W, T^k \rangle = \begin{cases} \dfrac{4e^{2\pi ki/L}}{\sqrt{L}(1 - e^{2\pi ki/L})} & k \text{ odd} \\ 0 & k \text{ even.} \end{cases}$$

If $k = \pm L/2$,

$$\langle W, T^{\pm L/2} \rangle = \begin{cases} -2/\sqrt{L} & L/2 \text{ is odd} \\ 0 & L/2 \text{ is even.} \end{cases}$$

Diametrically Opposite Pair

A current pattern D that uses only one current generator is given by

$$D_l = \begin{cases} 1 & l = L \\ -1 & l = L/2 \\ 0 & \text{otherwise.} \end{cases}$$

In this case,

$$\langle D, T^k \rangle = (1 - (-1)^k)/\sqrt{L} = \begin{cases} 2/\sqrt{L} & \text{if } k \text{ is odd} \\ 0 & \text{if } k \text{ is even.} \end{cases}$$

Adjacent Pair Pattern

A widely used current pattern F, introduced by the authors of [2], is one that uses a pair of adjacent electrodes to apply current:

$$F_l = \begin{cases} 1 & l = 1 \\ -1 & l = 2 \\ 0 & \text{otherwise.} \end{cases}$$

In this case, the inner product we need is

$$\langle F, T^k \rangle = (e^{ik\theta_1} - e^{ik\theta_2})/\sqrt{L}.$$

We now use these formulas to compute the size of the smallest conducting object we can detect in a body of radius $r^0 = 15$ cm. For related calculations, see [9], [10]. We take $L = 32$, $h = 3.6$ cm, $F = 10.6$ cm^2, $\sigma^0 = 1/(350\ \Omega\text{-cm})$, $\mu = 1$, and $f \approx 1$. We also assume that the precision of our system is such that the smallest voltage it can reliably measure is 1 mV in response to an applied current of 1 mA. (See Appendix C for details about the computations.)

CURRENTS WITH MAXIMUM MAGNITUDE 1 mA

current pattern	max. current density in mA/cm^2	power in μW	radius of smallest detectable object
B^+	0.094	7922	0.95
W	0.094	13540	0.84
D	0.094	238	2.7
F	0.094	85	8.6

We might draw two erroneous conclusions from this table: 1) it looks as if the Walsh pattern is better than the cosine pattern; and 2) the adjacent pair pattern seems to be a terrible one to use. However, this table does not allow us to make a fair comparison, because the Walsh pattern requires a great deal more power than the cosine, and the adjacent pair requires a great deal less. To make a realistic comparison, we should keep the power fixed.

CURRENTS WITH POWER 7.9 mW

current pattern	max. current density in mA/cm^2	power in mW	radius of smallest detectable object
B^+	0.094	7.9	0.953
$W/1.303$	0.072	7.9	0.958
$D/0.1730$	0.545	7.9	1.123
$F/0.1037$	0.909	7.9	2.576

This table illustrates the fact that the cosine pattern is the best for distinguishing a centered cylindrical object from a homogeneous background. It will not necessarily be the best, however, for objects that are not centered. A process for finding the best patterns for an unknown conductivity distribution is given in [10].

In Section II, we used the idea of distinguishability to predict that the trigonometric current patterns were best in this case. We can verify that the trigonometric patterns do indeed give the largest distinguishability.

To compute the distinguishability, we use (3.6) in the numerator of (2.3), which becomes

$$\sum_{l=1}^{L} |V_l - V_l^0|^2 = \|V - V^0\|^2 = \sum_{k=-L/2}^{L/2-1}{}' |\langle I, T^k \rangle|^2 (\rho_k - \rho_k^0)^2; \quad (3.9)$$

similarly, the denominator of (2.3) becomes

$$\sum_{l=1}^{L} I_l (V_l^0)^* = \langle I, V^0 \rangle = \sum_{k=-L/2}^{L/2-1}{}' |\langle I, T^k \rangle|^2 (\rho_k^0)^*. \quad (3.10)$$

Using (3.9) and (3.10) in (2.3), we finally obtain

$$\delta_P = \sqrt{\frac{\sum_{k=-L/2}^{L/2-1}{}' |\langle I, T^k \rangle|^2 (\rho_k - \rho_k^0)^2}{\sum_{k=-L/2}^{L/2-1}{}' |\langle I, T^k \rangle|^2 (\rho_k^0)^*}}. \quad (3.11)$$

In the following table, we compute δ_I and δ_P for a 2.5-cm radius conductor in the center of a 15-cm radius body. (See Appendix C for details.)

DISTINGUISHABILITIES

current pattern	δ_I in Ω	δ_P in $\Omega^{1/2}$
B^+	26.76	1.216
W	24.32	1.176
D	9.46	0.89
F	0.930	0.10

We see that either δ_I and δ_P is useful in deciding which current pattern is best for distinguishing a centered circular object.

APPENDIX A
SOBOLEV NORMS

The Sobolev norm [1], [22] is basically a delicate measure of the size and smoothness of a function. The smoothness of a function can be measured in terms of the number and size of the derivatives a function has. As we will see, smoothness can also be measured in terms of the Fourier representation.

A function defined on the unit circle S^1, for example, can be written in terms of its Fourier series as

$$f(\theta) = \sum_{n=-\infty}^{\infty} f_n e^{in\theta}. \quad (A.1)$$

Two derivatives with respect to theta can therefore be written

$$\partial_\theta^2 f(\theta) = \sum_{n=-\infty}^{\infty} -n^2 f_n e^{in\theta}. \quad \text{(A.2)}$$

If we want to require that $f - \partial_\theta^2 f$ be square integrable (i.e., in L^2), Parseval's identity [16] tells us that we could write this requirement as

$$\|f - \partial_\theta^2 f\|_0^2 = 2\pi \sum_{n=-\infty}^{\infty} (1 + n^2)^2 |f_n|^2 < \infty \quad \text{(A.3)}$$

where the norm on the left side is the usual L^2 norm, defined in (1.10). (Using the subscript zero makes this notation consistent with the definition (A.5) of the Sobolev norm below.) Requiring the left side of (A.3) to be finite forces f and its second derivative to be in L^2. This condition says (by definition) that f is in the Sobolev space $H^2(S^1)$. From the right side of (A.3), we see that this same condition can be expressed in terms of the Fourier coefficients of f. Thus, we see that smoothness, in the Sobolev sense, can be measured in terms of the decay of the Fourier coefficients.

This idea can be extended to include derivatives of fractional order: for any real s, we define the pseudodifferential operator

$$(1 - \partial_\theta^2)^{s/2} f = \sum (1 + n^2)^{s/2} f_n e^{in\theta}. \quad \text{(A.4)}$$

The Sobolev space $H^s(S^1)$ can be defined to be the space of functions f on the unit circle that satisfy the conditions that f and its derivatives up to order s are in $L^2(S^1)$. This requirement can be written

$$\|f\|_s^2 = \|(1 - \partial_\theta^2)^{s/2} f\|_0^2 = 2\pi \sum (1 + n^2)^s |f_n|^2 < \infty. \quad \text{(A.5)}$$

The left side of (A.5) defines the square of the Sobolev s-norm.

We see that the larger s is, the more derivatives of f are in L^2, or equivalently, the faster the Fourier coefficients f_n must decay in order to make the sum (A.5) converge. Rapid decay of the Fourier coefficients therefore translates into smoothness of the original function f. Thus, Sobolev spaces with larger indices are spaces of smoother functions. Similarly, if s is negative, the Fourier coefficients of f need not decay so fast. The more negative s is, the more singular an H^s function may be. If s is large and negative, the Fourier coefficients of f may actually grow, and the resulting Fourier series may not represent a function at all. In such a case, f can be interpreted as a generalized function or distribution [1], [22].

The above implies, in particular, that the $H^{1/2}$ norm of the voltage v is

$$\|v\|_{1/2}^2 = 2\pi \sum_{n=-\infty}^{\infty}{}' (1 + n^2)^{1/2} |v_n|^2. \quad \text{(A.6)}$$

We use the prime on the sum because v has no zeroth Fourier coefficient. Since

$$|n| \le \sqrt{1 + n^2} \le \sqrt{2}\,|n| \quad \text{(A.7)}$$

the $H^{1/2}$ norm of v is equivalent to expression (1.8) in the sense that

$$\sigma^0 \|v\|_{1/2}^2 / \sqrt{2} \le 2\pi \sum{}' \sigma^0 |n| |v_n|^2 \le \sigma^0 \|v\|_{1/2}^2.$$

Similarly, the $H^{-1/2}$ norm of j is

$$\|j\|_{-1/2}^2 = 2\pi \sum_{n=-\infty}^{\infty}{}' (1 + n^2)^{-1/2} |j_n|^2. \quad \text{(A.8)}$$

The $H^{-1/2}$ norm of j is equivalent to expression (1.7) in the sense that

$$\frac{1}{\sigma^0} \|j\|_{-1/2}^2 \le 2\pi \sum{}' \frac{|j_n|^2}{\sigma^0 |n|} \le \frac{\sqrt{2}}{\sigma^0} \|j\|_{-1/2}^2. \quad \text{(A.9)}$$

The reason equation (1.6) holds can now be understood as follows. We start with the expression for the power, use Parseval's relation [16], multiply and divide by $(1 + n^2)^{s/2}$, and finally use the Schwarz inequality:

$$\begin{aligned} \left| \int_S j v^* \right| &= \left| 2\pi \sum j_n v_n^* \right| \\ &= \left| 2\pi \sum \frac{j_n}{(1 + n^2)^{s/2}} (1 + n^2)^{s/2} v_n^* \right| \\ &\le \left(2\pi \sum \frac{|j_n|^2}{(1 + n^2)^s} \right)^{1/2} \\ &\quad \cdot \left(2\pi \sum (1 + n^2)^s |v_n^*|^2 \right)^{1/2}. \end{aligned}$$

For an arbitrary smooth surface S with no edges ("manifold without boundary"), the Sobolev space $H^s(S)$ can be defined in terms of the natural Laplacian ("Laplace–Beltrami" operator) for the surface S. Thus, $H^s(S)$ is defined to be the space of functions for which the norm

$$\|f\|_s = \|(1 - \nabla^2)^{s/2} f\|_0 \quad \text{(A.10)}$$

is finite.

The idea of using the Fourier representation of a function to interpret fractional derivatives can be extended to regions other than the unit circle. For example, if the region is $S = \mathbf{R}^n$, the fractional derivatives in (A.10) can be interpreted by writing f in terms of its Fourier transform:

$$f(x) = (2\pi)^{n/2} \int \hat{f}(\xi) \exp(i\xi \cdot x)\, d^n\xi. \quad \text{(A.11)}$$

By the Plancherel theorem [16], the Sobolev norm (A.10) can be written

$$\|f\|_s = \|(1 + |\xi|^2)^{s/2} \hat{f}(\xi)\|_0. \quad \text{(A.12)}$$

In the case when s is an integer and f is smooth, (A.10) can also be interpreted by recalling that ∇^2 is self-adjoint. Thus, (A.10) can be written

$$\|f\|_s = \int f (1 - \nabla^2)^s f^*.$$

In the case when $s = 1$, we can integrate by parts to obtain

$$\|f\|_1 = \int |f|^2 + \int |\nabla f|^2.$$

This suggests that if f is a function defined on a region B that has a boundary, the Sobolev $H^1(B)$-norm should be

$$\|f\|_1^2 = \|f\|_0^2 + \|\nabla f\|_0^2.$$

We do not discuss the definition of fractional order Sobolev spaces for regions with boundaries because the ideas are a little more complicated and are not needed in this paper.

Appendix B
Power as the Electrode Size Decreases

The ability of an impedance imaging system to distinguish between different conductivity distributions is limited not only by the measurement precision but also by the number of electrodes. This is because the best current densities may not be well approximated by current patterns for a small number of electrodes. Quantitative estimates of the errors in approximating continuum patterns by discrete ones are given in [14].

A large number of electrodes can be applied to a body only if the electrodes are small. Indeed, it is now possible, with present technology, to make a large number of very small electrodes. This appendix shows that as the electrode size becomes vanishingly small, the power required to push a fixed amount of current through them becomes arbitrarily large. The following calculation, which uses the "gap model" approximation to the current density [3], [14], [20], may be used in general to predict the power required to push fixed magnitude currents through an array of L electrodes when each electrode has area A.

In the "gap model" formulation, the current density is taken to be

$$j(\theta) = \begin{cases} I_l/A & \text{for } \theta \in e_l,\ l = 1, 2, \cdots, L \\ 0 & \text{otherwise,} \end{cases} \tag{B.1}$$

where A is the electrode area and e_l is the set of angles subtended by the lth electrode. We assume that the body is a cylinder of height h and radius r_0, with constant conductivity σ^0. For such a body, (1.1) and (1.2) can be solved by separation of variables, and the solution written in terms of the Fourier coefficients of the current density. For the gap model with equally spaced electrodes, each subtending an angle w, these Fourier coefficients are

$$j_n = \frac{1}{2\pi}\int j(\theta)e^{-in\theta}\,d\theta = \frac{1}{\pi}\sum_{l=1}^{L}\frac{I_l}{nA}e^{-in\theta_l}\sin\frac{nw}{2}. \tag{B.2}$$

The current density can be recovered from its Fourier coefficients by

$$j(\theta) = \sum_{n=-\infty}^{\infty}{}' j_n e^{in\theta}.$$

The voltages on the boundary are then

$$v^0(\theta) = \sum_{n=-\infty}^{\infty}{}' \frac{r_0}{\sigma^0|n|} j_n e^{in\theta}. \tag{B.3}$$

The gap model assumption is to take the voltage V_l^0 measured on the lth electrode to be $v^0(\theta_l)$ where $\theta_l = 2\pi l/L$ is the center of the lth electrode. Thus,

$$V_l^0 = \sum_{n=-\infty}^{\infty}{}' \frac{r_0}{\sigma^0|n|} j_n e^{in\theta_l}. \tag{B.4}$$

If we take the current pattern $I_l^k = \exp(ik\theta_l)$ where $k = -L/2, \cdots, -2, -1, 1, 2, \cdots, L/2$, insert (B.2) into (B.4) and use the fact [15] that

$$\sum_{l=1}^{L}\exp[i(k-n)2\pi l/L] = \begin{cases} L & \text{if } n = k + mL, \text{ where } m \text{ is an integer} \\ 0 & \text{otherwise.} \end{cases} \tag{B.5}$$

then we see that the voltage pattern corresponding to I^k is

$$\mathcal{R}^0 I^k = \rho_k^0 I^k \tag{B.6}$$

where ρ_k^0 is

$$\rho_k^0 = \frac{Lr_0}{\pi A\sigma^0}\sum_{m=-\infty}^{\infty}\frac{\operatorname{sgn}(k+mL)}{(k+mL)^2}\sin\frac{(k+mL)w}{2}. \tag{B.7}$$

Equation (B.6) shows that I^k is an eigenvector of $\mathcal{R}^0$. These eigenvectors we call the "characteristic current patterns," and the corresponding eigenvalues are the gap model "characteristic resistances." These characteristic resistances become infinite as the electrode area vanishes. This can be seen as follows.

Note that the area A of the electrode is related to its angular width w and its height h by $A = hr_0 w$. The angular width w, in turn, is related to the number L of electrodes as $w = 2\pi f/L$ where f is the fraction of the surface covered by electrodes. With these substitutions, we can rewrite (B.7) as

$$\rho_k^0 = \frac{1}{2\pi h\sigma^0}\sum_{m=-\infty}^{\infty}\frac{1}{|m+k/L|}\frac{1}{(m+k/L)\pi f}\cdot\sin[(m+k/L)\pi f]. \tag{B.8}$$

We split off into a separate ("main") sum those terms in (B.8) for which $(m + k/L)\pi f$ is between $-\pi/2$ and $\pi/2$, and the remainder sums. The integral test shows that these remainder sums are uniformly bounded. The "main" sum, on the other hand, diverges, which can be seen by the following argument. Since k/L is bounded by $1/2$, this sum will include as many terms as we want if we take f sufficiently small. For m in this range, however, $|\sin x| \geq 2|x|/\pi$. This "main" sum is therefore at least as large as the partial sum of $|m + k/L|$, a partial sum for the harmonic series. It can be made arbitrarily large by taking f sufficiently small. This shows that ρ_k^0 can be made arbitrarily large by taking the electrode width sufficiently small.

The power dissipated by the kth current pattern is proportional to

$$\langle I^k, \mathcal{R}^0 I^k \rangle = \rho_k^0 \| I^k \|^2.$$

If the magnitude of the currents is kept constant as the electrode size shrinks, the growth of ρ_k^0 causes the power to become arbitrarily large.

Appendix C

This appendix explains how the numbers in the tables were computed. The first table requires only evaluation of (3.5) and (3.6). To do this, we first simplify (3.5) by assuming that L is large. This enables us to neglect all the terms of $\rho_k^0 - \rho_k$ except the $m = 0$ one, because for $\Gamma < 1$, $\Gamma^{2k+L} << \Gamma^{2k}$. For essentially the same reason, in computing the voltage difference (3.6), we neglect all but the $k = \pm 1$ terms. These approximations give us the following formulas:

$$\max \delta V(B^+) \approx \frac{L}{\pi h \sigma^0} \frac{\mu\Gamma^2}{1 + \mu\Gamma^2}$$

$$\max \delta V(W) \approx \frac{4L}{\pi^2 h \sigma^0} \frac{\mu\Gamma^2}{1 + \mu\Gamma^2}$$

$$\max \delta V(D) \approx \frac{4}{\pi h \sigma^0} \frac{\mu\Gamma^2}{1 + \mu\Gamma^2}$$

$$\max \delta V(F) \approx \frac{4}{Lh\sigma^0} \frac{\mu\Gamma^2}{1 + \mu\Gamma^2}.$$

For the second table we need to compute the power. We do this by means of (3.10). In this computation, however, we cannot neglect all the terms with $|k|$ larger than 1. The power for each current pattern was obtained from a short BASIC program that performed the sum over k. A multiple of the square root of this power was used to normalize each pattern for the second table.

Acknowledgment

We are grateful to C. Caldwell and J. C. Newell for reading an early version of the manuscript carefully and making helpful comments. We would like to thank D. G. Gisser, J. C. Goble, J. C. Newell, and G. Saulnier, whose collaboration in building impedance imaging systems continues to inspire and enlighten us.

References

[1] R. A. Adams, *Sobolev Spaces*. New York: Academic, 1975.
[2] D. C. Barber and B. H. Brown, "Applied potential tomography," *J. Phys. E. Sci. Instrum.*, vol. 17, pp. 723-733, 1984.
[3] K.-S. Cheng, D. Isaacson, J. C. Newell, and D. G. Gisser, "Electrode models for electric current computed tomography," *IEEE Trans. Biomed. Eng.*, vol. 36, pp. 918-924, 1989.
[4] M. Cheney, D. Isaacson, J. C. Newell, J. C. Goble, and S. Simske, "NOSER: An algorithm for solving the inverse conductivity problem," *Internat. J. Imaging Syst. Technol.*, vol. 2, pp. 66-75, 1990.
[5] R. Courant and D. Hilbert, *Methods of Mathematical Physics, Vol. 1*. New York: Interscience, 1937.
[6] W. Daily, W. Lin, and T. Buscheck, "Hydrological properties of Topapah Spring tuff: Laboratory measurements," *J. Geophys. Res.*, vol. 92, pp. 7854-7864, 1987.
[7] L. F. Fuks, M. Cheney, D. Isaacson, D. G. Gisser and J. C. Newell, "Detection and imaging of electric conductivity and permittivity at low frequency," *IEEE Trans. Biomed. Eng.*, vol. 38, pp. 1106-1110, 1991.
[8] P. Grisvard, *Elliptic Problems in Nonsmooth Domains*. Boston: Pitman, 1985.
[9] D. G. Gisser, D. Isaacson, and J. C. Newell, "Current topics in impedance imaging," *Clin. Phys. Physiol. Meas.*, vol. 8, Suppl. A, pp. 39-46, 1987.
[10] D. G. Gisser, D. Isaacson, and J. C. Newell, "Theory and performance of an adaptive current tomography system," *Clin. Phys. Physiol. Meas.*, vol. 9, suppl. A, pp. 35-41, 1988.
[11] ——, "Electric current computed tomography and eigenvalues," *SIAM J. Appl. Math.*, vol. 50, pp. 1623-1634, 1990.
[12] D. Isaacson, "Distinguishability of conductivities by electric current computed tomography," *IEEE Trans. Med. Imag.*, vol. MI-5, pp. 91-95, 1986.
[13] D. Isaacson and M. Cheney, "Current problems in impedance imaging," in *Inverse Problems in Partial Differential Equations*, D. Colton, R. Ewing, and W. Rundell, Eds. Philadelphia: SIAM, 1990.
[14] ——, "Effects of measurement precision and finite numbers of electrodes on linear impedance imaging algorithms," *SIAM J. Appl. Math.*, vol. 51, pp. 1705-1731, 1991.
[15] E. Isaacson and H. B. Keller, *Analysis of Numerical Methods*. New York: Wiley, 1966.
[16] Y. Katznelson, *An Introduction to Harmonic Analysis*. New York: Dover, 1976.
[17] J. P. Keener, *Principles of Applied Mathematics*. New York: Addison-Wesley, 1988.
[18] J. C. Newell, D. G. Gisser, and D. Isaacson, "An electric current tomograph," *IEEE Trans. Biomed Eng.*, vol. 35, pp. 828-833, 1988.
[19] A. D. Seagar and R. H. T. Bates, "Full-wave computed tomography, Part 4: Low frequency electric current CT," *IEE Proc.*, vol. 132A, pp. 455-466, 1985.
[20] E. Somersalo, M. Cheney, and D. Isaacson, "Electrode models for electric current computed tomography," *SIAM J. Appl. Math.*, in press.
[21] A. D. Seager, T. S. Yeo, and R. H. T. Bates, "Full-wave computed tomography, Part 2: Resolution limits," *IEE Proc.*, vol. 131A, pp. 616-622, 1984.
[22] F. Treves, *Basic Linear Partial Differential Equations*. New York: Academic, 1975.

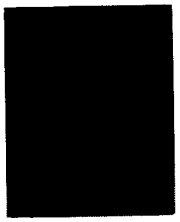

Margaret Cheney received the B.A. degree in mathematics and physics from Oberlin College, Oberlin, OH, in 1976, and the Ph.D. in mathematics from Indiana University; Bloomington, in 1982.

She was a postdoc at Stanford University, Stanford, CA, from 1982 to 1984 and an assistant professor of mathematics at Duke University, Durham, NC, from 1984 to 1988. For the 1987-1988 academic year, she was on leave at New York University's Courant Institute. Since 1988, she has been an associate professor of mathematics at Rensselaer Polytechnic Institute, Troy, NY. Most of her work has been on the inverse problems that arise in quantum mechanics, acoustics, and electromagnetic theory.

Dr. Cheney has received several awards, including the Office of Naval Research Young Investigator Award in 1986 and a National Science Foundation Faculty Award for Women in Science and Engineering in 1990.

David Isaacson (M'86) received the Ph.D. degree in mathematics from New York University's Courant Institute of Mathematical Sciences in 1976.

From 1976 to 1980 he was an Assistant Professor of mathematics at Rutgers University, New Brunswick, NJ. Since 1980 he has been at Rensselaer Polytechnic Institute, where he is Professor of Mathematics and Computer Science. He is currently working on problems arising in the use of electromagnetic fields for the diagnosis and treatment of disease.